crystals

MDPI

Article

The Effect of Ultrasound on the Crystallisation of Paracetamol in the Presence of Structurally Similar Impurities

Thai T. H. Nguyen [1], Azeem Khan [1], Layla M. Bruce [1], Clarissa Forbes [1,2,3], Richard L. O'Leary [2] and Chris J. Price [1,3,*]

1 Department of Chemical & Process Engineering, University of Strathclyde, Glasgow G1 1XQ, UK; thai.nguyen@strath.ac.uk (T.T.H.N.); rfcazeem@gmail.com (A.K.); layla.mir-bruce@strath.ac.uk (L.M.B.); clarissa.forbes@strath.ac.uk (C.F.)

2 The Centre for Ultrasonic Engineering, Department of Electronic & Electrical Engineering, University of Strathclyde, Glasgow G1 1XW, UK; richard.o-leary@strath.ac.uk

3 EPSRC Centre for Continuous Manufacturing and Crystallisation, University of Strathclyde, Glasgow G1 1RD, UK

* Correspondence: chris.price@strath.ac.uk

Academic Editor: Judy Lee
Received: 17 August 2017; Accepted: 26 September 2017; Published: 30 September 2017

Abstract: Sono-crystallisation has been used to enhance crystalline product quality particularly in terms of purity, particle size and size distribution. In this work, the effect of impurities and ultrasound on crystallisation processes (nucleation temperature, yield) and crystal properties (crystal size distribution determined by Focused Beam Reflectance Measurement (FBRM), crystal habit, filtration rate and impurity content in the crystal product by Liquid Chromatography-Mass Spectroscopy (LC-MS)) were investigated in bulk suspension crystallisation experiments with and without the use of ultrasound. The results demonstrate that ultrasonic intervention has a significant effect on both crystallisation and product crystal properties. It increases the nucleation rate resulting in smaller particles and a narrower Particle Size Distribution (PSD), the yield has been shown to be increase as has the product purity. The effect of ultrasound is to reduce the level acetanilide impurity incorporated during growth from a 2 mol% solution of the selected impurity from 0.85 mol% to 0.35 mol% and likewise ultrasound reduces the uptake of metacetamol from 1.88 mol% to 1.52 mol%.

Keywords: suspension crystallisation; impurities; crystal size distribution; filtration rate; optical microscopy; image analysis; crystal morphology; purification; HPLC; ultrasound intensity

1. Introduction

Crystallisation is the principal purification technique in the pharmaceutical, fine chemical, paint, pigments and agrochemical sector. It allows the desired product to be obtained in a pure state leaving unwanted or hazardous impurities in solution where they can be removed effectively by filtration and washing. During crystallisation, molecules of the product assemble together to form crystals with a regular 3D packing arrangement known as a crystal lattice. Purification occurs by molecular recognition at the solution-lattice interface. The mismatch between some impurity molecules and the crystal lattice is so significant that the impurity molecule cannot be incorporated in the lattice and is rejected. However, if the molecular mismatch is small enough, the impurity molecule can become incorporated into the crystal lattice. If the portion of the impurity molecule projecting out from the crystal surface is different from the adjacent molecules in the surface layer of the crystal this is likely to disrupt and retard subsequent growth at that growth site and adjacent sites on that crystal face.

Increasing the crystallisation driving force, i.e., increasing supersaturation level, reduces selectivity allowing easier incorporation of the impurity into the crystal lattice and subsequent overgrowth. In one of the author's industrial experience, typical feed streams to industrial crystallisation contain several mole% of impurities so interactions between impurity molecules and the growing crystal surface are very frequent and can have undesirable consequences. Impurity poisoning of growing crystal faces increases processing time and slows the approach to equilibrium. In some instances, a significant amount of product has to be left in solution and lost in the waste stream in order for the process to be run with a plausible batch duration. Sometimes the product is so impure that it has to be re-crystallised to meet the required specification.

Most impurities that are readily incorporated into the growing crystal lattice and act as crystal growth inhibitors are close analogues of the active pharmaceutical ingredient and are produced inadvertently as by-products or degradants during the synthetic process. As well as retarding crystal growth they also modify crystal habit. As a consequence, other attributes of the isolated crystals such as bulk density and powder flow are modified and can influence both the subsequent formulation process and drug product performance. Several routes have been identified [1] by which impurities become entrapped in final crystalline product: (i) Deposition on crystal surfaces due to the incomplete removal of impure mother liquor during filtration and washing; (ii) incorporation within the crystal lattice by molecular recognition/substitution or (iii) entrapment of multiple impurity molecules within inclusions or between individual crystallites in agglomerates. The impact of specific impurities on crystallisation processes depends on; the structure of the impurity, its concentration, the crystallisation solvent, the supersaturation and the temperature of the crystallising solution. The presence of impurities during the crystallisation process can significantly modify the kinetics of nucleation, the growth rate of specific crystal faces, crystal morphology (habit) and the polymorphic phase crystallized. These undesired effects can cause costly delays during the research and development process within the pharmaceutical industry. There are many case studies of impurity effects reported in the crystallisation literature [2–5]. The effect of increasing amounts of the impurity p-acetoxyacetanilide on paracetamol nucleation is to increase the metastable zone width and lengthen the induction time [3,6,7]. It has been reported that this due to its ability to disrupt the formation and growth of the critical nucleus [3,8]. Impurities have been reported both to suppress and occasionally to accelerate crystal growth processes [9]. N-phosphonomethyl phosphoric acid (PMG) crystallisation is reported to be affected by the impurities, iminobismethylene phosphonic acid and amino methyl phosphoric acid by selective absorption onto the (100) face inhibiting the growth of this face; while the impurity N-phosphonomethyl iminodiacetic acid (PIDA) does not change crystal habit noticeably [10]. Also, an impurity has been reported to affect the solution-mediated phase transformation of the metastable A form to the stable B form of an active pharmaceutical ingredient [11]. The presence of impurities is widely reported to influence crystal growth and crystal morphology [9,12–15]. This is the case for amino acids on the habit of glycine crystals [16], or urea crystallisation in the presence of biuret [15]. The change of crystal habit is due to a difference in the extent of adsorption and magnitude of binding energies on different crystal faces [16]. For this reason, identification, quantification and reduction of impurities in the early stages of synthetic process development can avoid problems in crystallisation development, enhance product performance and reduce development time [17].

Ultrasound (US) has been used in the chemical and food industries to enhance crystalline product quality in terms of particle size, size distribution and impurity and is termed sono-crystallisation. Ultrasound has been widely reported to influence the primary nucleation process accelerating nucleation kinetics, this is typically expressed in terms of reducing the induction time and MSZW [18–33]. Ultrasound can also increase the rate of secondary nucleation, this is manifested as a reduction on the product crystal size distribution [20,22,24,31,32,34–43]. Ultrasound can also influence crystal growth [20,25,26,36,40,44–46] although the effect on crystal growth is not as dramatic as on nucleation and arises largely from enhanced mass transfer [46] and can influence crystal morphology. Other reported outcomes of ultrasonic intervention include influencing;

which polymorph nucleates [23,47,48], crystal structure [30], crystal properties [49] and reaction crystallisation [45]. Several proposed mechanisms of the effect of ultrasound on crystallisation have been published. These include the formation of local hot spots which arise from the large energy release on the collapse of cavitation bubbles creating highly localised regions of extremely high temperature and pressure [50,51], or due to rapid cooling which follows; shockwaves released from cavitation bubbles [52,53], promoting mass transfer and collisions between crystals and adjacent surfaces [54]. These effects of ultrasound on crystallisation have been demonstrated on pharmaceuticals and commodity chemicals including; lactose [35,39,42,55], alpha-dextrose monohydrate [20], glycine [48], p-aminobenzoic acid [47], adipic acid [28], benzoic acid [31], acetylsalicylic acid [27], protein [19] various food products [30,56,57] and in the crystallisation of inorganic materials such as potassium sulphate [26], potassium dihydrogen phosphate [32] and calcite [34]. Ultrasound has also been utilized in continuous crystallisation [28,58–60]. While some authors mention that ultrasound can improve crystal purity [54]; there is very limited data on the effect of ultrasound on the purity of the final crystalline product. This work focuses on the use of ultrasound in suspension crystallisation processes to improve product purity, yield and crystal size distribution. The objective is to develop a bulk suspension sonocrystallisation process at lab scale which exploits ultrasound to improve product purity, yield and crystal habit. The research hypothesis is that through active intervention in the molecular processes occurring at growing surfaces it may be possible to remove impurity molecules from the surfaces and reduce the entrapment of impurities inside agglomerates formed during growth. These measurements aim to increase understanding of how ultrasonic interventions affect product purity both directly through influencing impurity incorporation during growth and indirectly through influencing nucleation kinetics, crystal size distribution and agglomeration, which all influence the purity of final products by modifying the extent to which impurities are removed during filtration and washing.

Paracetamol (Acetaminophen) has been used as a model compound for this study because its crystallisation behaviour is well characterised [2–5] and multiple structurally related impurities are readily available. Three polymorphs of paracetamol have been reported [61–63] but so far only forms I and II have been obtained as single crystals which have allowed the crystal structure to be solved. Polymorph I (monoclinic, P21/n) is the thermodynamically stable form at room temperature, this can be prepared as large single crystals from solutions in various solvents. Polymorph II (orthorhombic, Pcab) is metastable at ambient conditions. Crystals of paracetamol form I exhibit three dominant crystal habit faces; {100}, {001} and {110}. Individual paracetamol crystals exhibit different crystal habits, for example significant changes of the growth rate and resultant morphology of paracetamol single crystals are observed in pure [64] and impure systems [4].

2. Materials and Methodology

2.1. Materials

Paracetamol (BioXtra grade, purity $\geq$ 99.0%, Lot number 637515L263) was obtained from Sigma-Aldrich (St. Louis, MO, USA). The impurities investigated were Acetanilide 99.0% Lot number STBD0193V and Metacetamol 97.0% Lot number MKBX4643V both also obtained from Sigma-Aldrich, all three samples were analysed on receipt to confirm the reported assay. The basis for selecting acetanilide is that it is structurally similar to paracetamol but lacks the hydroxyl group and so while it may be incorporated into the crystal lattice it is deficient in a hydrogen bonding opportunity. Metacetamol was selected as a positional isomer which is also likely to be incorporated into the crystal lattice; however, the misplaced hydroxyl group is likely to disrupt the local hydrogen bonding arrangement. Importantly both are more soluble than paracetamol in 3-methyl-1-butanol, the selected solvent ensuring little risk of them crystallizing independently during the experiments.

The crystallisation solvent 3-methyl-1-butanol (isoamyl alcohol) was selected because the solubility relationship with temperature for paracetamol is appropriately steep over the chosen

temperature range and the product crystals tend not to form agglomerates. 3-methyl-1-butanol was obtained from Sigma-Aldrich 98%, n-heptane 99% from Alfa Aesar (Ward Hill, MA, USA) used for filter cake washing following filtration. HPLC grade methanol and water used for the analysis were purchased from Sigma-Aldrich.

2.2. Equipment Apparatus

2.2.1. Solubility Measurements

Gravimetric Method

In order to evaluate the effect of impurities on the crystallisation of paracetamol it was first necessary to measure the extent to which the impurities affect the solubility of paracetamol in the crystallisation solvent. Solubility measurements were performed by equilibration using a Stuart SI60D Incubator (Stuart, Staffordshire, UK). Agitation of the equilibrating samples was provided by a Thermo scientific submersible telesystem 15.20 magnetic stirrer plate (Thermo Fisher Scientific, Waltham, MA, USA). The temperature was recorded using an Omega HH800SW temperature sensor (Omega, Manchester, UK). Samples were taken using an Eppendorf pipette weighed on an A&D GR series balance (A&D Instruments Limited, Manchester, UK) and evaporated to dryness in a Memmert GmbH vacuum oven V0200 (Memmert GmbH + Co. KG, Schwabach, Germany) at 55 °C.

Detection of the Dissolution Temperature Method Using Crystalline-Technobis Crystallisation Systems

Solubility measurements of acetanilide and metacetamol were also conducted in a Technobis Crystalline system, a multi-reactor crystallisation platform which has eight independent Peltier heater-coolers able to maintain temperatures from −15 °C to 150 °C. Each 8 mL (34 × 10 mm) crystallizer is equipped with a three-blade marine impeller with overhead stirring. Each vessel position is equipped with a turbidity sensor and a camera allowing turbidity and images to be recorded and synchronised with the temperature time profile.

2.2.2. Sono-Crystallisation Studies

A schematic diagram of the experimental equipment used to evaluate the effect of ultrasound on crystal purity is shown in Figure 1. The system comprised two cell culture flasks, double side arm, Celstir® 125 mL placed onto a submersible Telesystem 15.20 stirrer from Thermo Scientific (Waltham, MA, USA) immersed in a XUB25 ultrasonic bath from Grant Instruments (Cambridge, UK) operating at 35 ± 3 kHz. The temperature of the water in the ultrasonic bath and hence the solutions in the Celstir® flasks was controlled using an Immersion Compact Thermostat (ICC) from IKA (Staufen im Breisgau, Germany) which was connected to a Hailea HC-150A chiller (GuangDong, China). Additional cooling capacity was provided by a stainless-steel dip coil running around the base of the ultrasonic bath and connected to a Lauder LCK1913, ECO RE 420G thermocirculator (Lauda Brinkmann, NJ, USA). The temperature of solutions was monitored using a precise PPL-GMH-3750 thermometer and Pt100 probe (±0.03 °C) (GHM Messtechnik GmbH Standort Greisinger, Regenstauf, Germany). The point of nucleation was determined by visual observation, initially a few particles were observed and the solution gradually became cloudy. On completion of the crystallisation (~3–3.5 h after nucleation process occurs) the product crystal size distribution was measured in situ by Focused Beam Reflectance (FBRM) (Mettler Toledo, Greifensee, Switzerland). The product suspension was filtered using a Vac Master 10 system (Biotage Ltd., Uppsala, Sweden) which had been modified to accommodate 50 mL graduated cylinders which allowed the filtration rate to be measured, filtration to be halted at dry land, and the mother liquor and individual wash liquors to be segregated for subsequent assay. The filtration driving force was monitored and controlled using a Büchi V800 vacuum controller (Büchi UK Ltd., Oldham, UK).

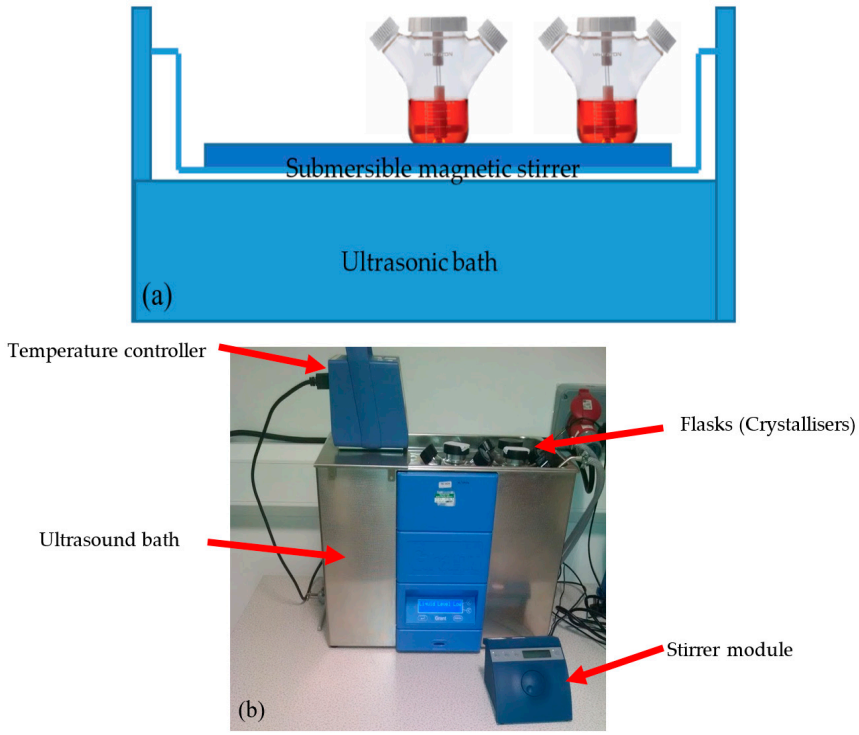

Figure 1. (**a**) Schematic diagram and (**b**) Annotated photograph showing the experiment setup for suspension cooling crystallisation of paracetamol in the presence of impurities using an ultrasonic bath.

Chemical analysis of product crystals, mother liquors and wash liquors was performed using an Agilent High Performance Liquid Chromatography 6130 dual source model (Agilent, Santa Clara, CA, USA) provided with a thermostated autosampler, a thermostated column compartment and a single wavelength ultraviolet (UV) detector and a 2.7 µm Poroshell 120 EC-C18 Column: 4.6 × 75 mm to determine the crystalline product purity.

2.3. Experimental Method

2.3.1. Solubility

Gravimetric Method

Solubility measurements were performed by equilibration using a Stuart SI60D Incubator operated over the temperature range 25 to 50 °C. The sample size employed to prepare saturated solutions to determine solubility was 15 mL. The effect of impurities on solubility was determined by dissolving a known target amount of metacetamol and/or acetanilide in the solvent prior to the addition of paracetamol. Individual vials were prepared with specific impurity loadings and then equilibrated with an excess of paracetamol. The vials were placed onto a Thermo scientific submersible telesystem 15.20 magnetic stirrer plate and agitated at 190 rpm. The temperature was kept within ±0.2 °C of the desired temperature which was recorded with an Omega precise thermocouple. After equilibration for 24 h, the excess solid paracetamol was allowed to settle for 1 h without agitation. A 2 mL sample of the clear saturated solution was withdrawn using an Eppendorf pipette taking great care not to disturb the settled solids. The samples were then transferred into a labelled and weighed vial. The sample vial containing the saturated solution was weighed immediately. This sampling process was repeated for each equilibrated vial and the samples were placed in a fume hood and allowed to evaporate to dryness for 24 h, after evaporation the samples, were then transferred to a vacuum oven and allowed to dry for a further 48 h at 55 °C. The dry residue mass, was determined and the solubility, expressed in mg of solute/g of solvent, was calculated with subtraction of the known amount of impurity in the

dry samples based on the presumption that the impurity remained evenly distributed throughout the liquid phase.

Dissolution Temperature Detection Method

A series of suspensions of known concentration of metacetamol (50–130 mg/g) and acetanilide (80–200 mg/g) in 3-methyl-1-butanol were prepared in 8 mL vials. The vials were heated from 5 °C to 70 °C at heating rate 0.1 °C/min. The temperature of dissolution was determined at the point at which all the particles were completely dissolved. By making measurements across a range of compositions the solubility curve was determined and the solubility at specific temperatures within this range can be interpolated.

2.3.2. Ultrasonic Intensity Measurements

The sonomechanical activity from the XUB25 ultrasonic bath was characterised by measurement of acoustic intensity using a NH4000 PVDF needle hydrophone (Precision Acoustics Ltd., Dorset, UK). The experimental arrangement was as shown in Figure 1 except the lid of the Celstir vessel was replaced with a plug manufactured from PVC that allowed the needle hydrophone to be positioned 25 mm from the base of the Celstir vessel, aligned with the central axis of the same. In order to make measurement of acoustic intensity within the Celstir vessel, the time domain waveform from the NH4000 hydrophone was recorded with an Agilent Technologies InfinniVision X2024-A digital oscilloscope (Agilent Technologies, South Queensferry, UK). A timing trigger for the measurement was provided via a submersible piezoelectric transducer, sensitive at the operating frequency of the XUB25 bath, and positioned on the top surface of the stirrer plate.

Prior to starting the measurements, the NH4000 hydrophone was wetted and soaked for 1 hour in deionised water. As was described in Section 2.3.3, the crystallisation was undertaken using organic solvent which is incompatible with the PVDF hydrophone tip. In order to protect the hydrophone tip during the measurement of the acoustic intensity in the crystallisation medium, the hydrophone was placed inside an 8 mm diameter latex rubber sheath filled with deionised water. The Celstir vessel used for suspension crystallisation experiments was filled with an aliquot of the crystalisation solvent; the hydrophone, complete with protective sheath, was immersed into the crystallisation medium as shown in Figure 2. Measurements of acoustic intensity were then undertaken with the crystallisation vessel placed inside the XUB25 bath, it was located around the defined positions on the stirrer plate at the bottom of the ultrasonic bath—all measurements were recorded at 30 °C. The peak instantaneous acoustic intensity of the recorded waveform was determined at both 50% and 100% power setting on the XUB25 bath.

Figure 2. Photograph of the hydrophone arrangement within the Celstir vessel set-up for ultrasonic intensity measurement.

2.3.3. Sono-Crystallisation

A 150 mL suspension containing 12.65 g of paracetamol and 1% or 2% mol of metacetamol and/or acetanilide in 115 g 3-methyl-1-butanol was prepared in cell culture flasks, Celstir® 125 mL. The paracetamol suspension in 3-methyl-1-butanol with the presence of impurities, was immersed and sonicated in the ultrasonic bath, XUB25, operating at 35 ± 3 kHz and was continuously stirred at a rate of ~150 rpm using a submersible Telesystem 15.20. The solution was heated to 65 °C and held at 65 °C for 15 min to ensure complete dissolution which was verified by visual inspection before slow cooling to 15 °C over 2 h. During the cooling crystallisation process, the nucleation temperature of the solutions was recorded. At the end of the crystallisation (3 h after nucleation) and immediately prior to isolation, the crystal size distribution was measured in situ using an FBRM to determine the mean chord length distribution. Then the product crystals were separated from the mother liquors using the modified VacMaster 10 system at pressure driving force of 200 mbar using a 70 mL Isolute filter tube with a polyethylene filter with a nominal pore size of 10 µm (Biotage Ltd., Uppsala, Sweden). The time required to collect filtrate volumes of 5 mL, 10 mL, 15 mL etc. were recorded. The filtration was halted at "dry land" the point where the filter cake surface is first exposed above the mother liquors. The mass of the solvent wet cake was measured. From the filtration data, the filtration rate and filter cake resistance were obtained using Darcy's equation [65].

$$\frac{dt}{dV} = \frac{\mu\alpha C}{\Delta P A^2} V + \frac{\mu R_m}{A \Delta P} \quad (1)$$

where: t is time (s); V is volume (m^3); α is cake resistance (m/kg); μ is the mother liquor viscosity (kg/s.m); ΔP is pressure difference (Pa); C is concentration of solids (kg/m^3); A is area of cake (m^2); R_m is resistance of filter medium (m^{-1}).

In this work, filtration was carried out at constant pressure difference, ΔP = 200 mbar. Integration Darcy's equation gives:

$$\frac{t}{V} = \frac{\mu\alpha C}{2\Delta P A^2} V + \frac{\mu R_m}{A \Delta P} \quad (2)$$

Plotting t/V versus V will allow the cake resistance α to be determined.

The ratio of the concentration of impurity in the product crystals to the concentration of impurity relative to paracetamol in the mother liquors was also determined by dissolution of product crystals and HPLC Analysis.

2.3.4. Impurity Analysis Using HPLC

The separation of analytes was achieved using an Agilent Poroshell column operated at 40 °C with an isocratic elution of 1 mL/min, the mobile phase composition was 80% water and 20% methanol. The detection wavelength was 243 nm, which represents the maximum absorbance for both paracetamol and metacetamol [66] while still remaining close to the lambda max for acetanilide at 242 nm [67]. The material corresponding to each peak in the chromatogram was identified using mass spectroscopy. The analytical sample used to determine the purity of the product crystals was prepared by weighing 14 mg of dry product crystals into a 100 mL volumetric flask and dissolving them in a 5% methanol/95% water mixture to prepare a solution with a concentration which was within the concentration range used to calibrate the instrument. Mother liquors were similarly diluted by mass to ensure appropriate composition for assay.

3. Results

3.1. Solubility

The solubility curves of paracetmol, metacetamol and acetanilide in 3-methyl-1-butanol prepared using the isothermal equilibration and gravimetric analysis and polythermal dissolution temperature detection method are shown in Figure 3. These data are summarised in Table 1. Full details of

the gravimetric studies and dissolution temperature detection are given in Section S1 within the ESI† materials.

The solubility of paracetamol, metacetamol and acetanilide increase with increasing temperature. Paracetamol is the least soluble in 3-methyl-1-butanol and acetanilide is the most soluble and exhibits the strongest dependency on temperature (Figure 3). Examining the data presented in Figure 3, there was a discrepancy in solubility of metacetamol obtained by isothermal equilibration followed by gravimetric analysis and by observing the dissolution temperature during heating using the Technobis Crystalline. Determining the dissolution temperature using the Crystalline involves identifying a clear point at which dissolution is presumed to have occurred. The clear point was determined using both transmissivity measurement and examining images from the crystalline camera. The dissolution kinetics depend on the size and shape of the crystals dissolving and their ability to impede the passage of light (transmissivity) or to be clearly resolved in an image (camera based measurement). Although the measurement was performed at a modest heating rate of 0.1 °C/min, the possibility of overshooting the dissolution temperature remained. Metacetmol has a very thin needle-like crystal morphology; the crystals appear to persist some while after they could have dissolved in an isothermal experiment. As a result complete dissolution is detected at slightly higher temperature than seen in the gravimetric method. Interestingly, there is no similar discrepancy in the data collected using the two methods for acetanilide, this is believed to be due to the higher solubility of acetanilide and the more rapid dissolution which may be linked to the thin plate-like crystal habit.

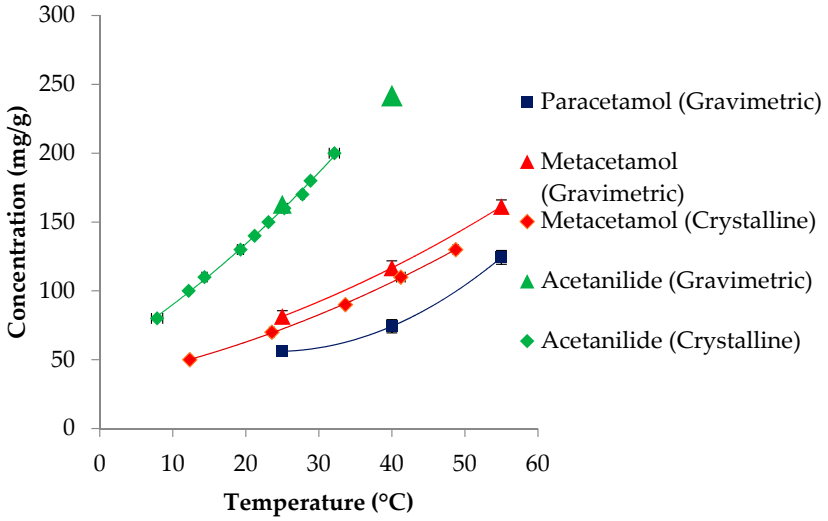

Figure 3. Solubility of paracetamol, metacetamol and acetanilide in 3-methyl-1-butanol obtained by isothermal equilibration followed by gravimetric analysis and by observing the dissolution temperature during heating using the Technobis Crystalline.

Table 1. Molecular weights, melting points, enthalpy of fusion and measured solubilities of paracetamol, metacetamol and acetanilide determined using the gravimetric method.

Compounds	Molecular Weight (g/mol)	Melting Point (K)	ΔH_{fusion} (kJ mol^{-1})	Measured Solubility in 3-methyl-1-butanol (mg/g)		
				25 °C	40 °C	55 °C
Paracetamol	151.16	443.6 [68]; 442.9 [69]	27.1 [68]; 30.72 [69]	54.8	74.3	124.3
Metacetamol	151.16	420 [70,71]	26.0 [71]; 28.8 [70]	81.4	116.7	162.6
Acetanilide	135.17	387.5 [69]	20.30 [69]	162.8	241.8	-

The solubility of a crystalline organic material typically depends on the lattice structure (polymorph), melting point, molecular weight and solvent choice. The measured solubility of paracetamol and metacetamol are relatively similar in comparison with acetanilide, this is consistent

with their relationship as positional isomers containing the same functional groups. The paracetamol crystal structure is dominated by hydrogen-bonded molecular chains packed in a 'herring bone' pattern. Similarly, metacetamol crystals are bound together by a network of hydrogen bonding interactions. Acetanilide however has no hydroxyl group in the para-position so lacks a proton donor. In addition, the melting point and the enthalpy of fusion decrease in the order Paracetamol > Metacetamol > Acetanilide (see Table 1). For acetanilide the crystal structure is such that molecules are bound by weaker forces than in paracetamol due to lack of the hydroxyl group reducing the opportunity to form a hydrogen bonding network. Acetanilide has a substantially lower heat of fusion and a lower melting point than paracetamol and metacetamol. The relative solubility is presumed to affect the impurity segregation of the final crystalline product.

The data presented in Figure 4 indicate that the presence of 1–4% of the selected impurities does not significantly affect the solubility of paracetamol. At 25 °C and 40 °C, it was shown that the solubility is similar or increases slightly with the presence of the selected impurities. At 55 °C, the data shows increased scatter and the trend is less pronounced. It can be concluded that the effect of 1–4% metacetamol/acetanilide on the solubility of paracetamol is modest.

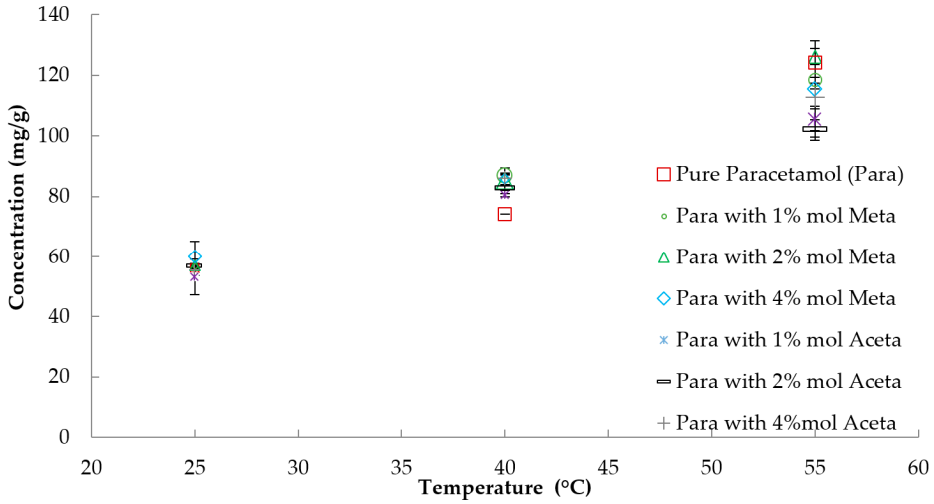

Figure 4. Solubility of paracetamol in 3-methyl-1-butanol with the presence of impurities (metacetamol and acetanilide) obtained by equilibration and gravimetric assay.

3.2. Ultrasonic Intensity Measurements

The ultrasound intensity measurements reveal that the local ultrasonic field is highly chaotic and intensities range from 0.12 to 0.25 mW/cm^2 at 50% ultrasonic power and from 0.9 to 1.68 mW/cm^2 at 100% power (see Table 2). It is clear from this data that the % ultrasound power is not a linear descriptor. Crystallisation experiments were conducted at positions 1 and 2 and the ultrasound intensity applied during these experiments can be characterised as; zero (0 mW/cm^2) low, 50% ultrasound power (0.19 ± 0.06 mW/cm^2) and high, 100% ultrasound power (1.45 ± 0.21 mW/cm^2).

Table 2. The ultrasonic intensity was measured at four positions within the ultrasonic bath.

Positions on the Stirrer plate at the Bottom of the Ultrasonic Bath	Ultrasonic Intensity (mW/cm^2)	
	50% Ultrasonic Power	100% Ultrasonic Power
1	0.13 ± 0.02	1.25 ± 0.13
2	0.25 ± 0.03	1.68 ± 0.25
3	0.24 ± 0.02	1.32 ± 0.09
4	0.12 ± 0.04	0.9 ± 0.07
Average values	0.19 ± 0.07	1.29 ± 0.32

3.3. Sonocrystallisation

The data comprise 11 suspension crystallisation experiments designed using the Design of Experiments software MODDE. (Umetrics Modde, Version 11, MKS Instruments, Umea, Sweden) to facilitate multivariate analysis. A full factorial (2 level) method was used to create a data set that was then analyzed using multiple linear regression (MLR) methods to measure effects of the three independent variables on the experimental responses. The parameters investigated were; the concentrations of the two impurities where the parameter range was selected as 0–2 mol% and ultrasonic power where the parameter range was 0% to 100% power settings on the ultrasonic bath. When the ultrasonic power was measured the center point (50% ultrasound power) the intensity was found to be 0.19 ± 0.06 mW/cm^2 and at 100% ultrasound power the intensity was 1.45 ± 0.21 mW/cm^2. The responses analyzed were nucleation temperature, particle size, filtration rate, product yield and the percentage of impurities in the product crystals.

The effect of the percentage of impurities present in solution at the start of crystallisation and ultrasonic power on; nucleation temperature, crystal size distribution, filtration rate and process yield at a defined crystallisation end point are summarised in Table 3.

Table 3. Summary of crystallisation temperature, crystal size distribution, filtration time (for 50 mL suspension solution), filtration rate, cake resistance and process yield as a function of the percentage of impurities and ultrasonic power.

Experiments	T_{crys} (°C)	PSD Mean Chord Length (μm)	Filtration Time (s)	Filtration Rate (m^3/s)	Cake Resistance (m/kg)	Yield
Pure paracetamol (100% power US)	41.3	47–55	209	1.90×10^{-7}	7.03×10^{11}	57.7%
Pure paracetamol (no US)	36.0	85–100	95	$4.29 \times 1\,0^{-7}$	2.62×10^{9}	54.3%
2 mol% Metacetamol (100% power US)	36.4	47	361	1.07×10^{-7}	1.52×10^{10}	45.5%
2 mol% Metacetamol (no US)	After maintaining at 15 °C for approx. 1.5 h	100–109	45	1.06×10^{-7}	9.02×10^{8}	39.1%
2 mol% Acetanilide (US 100%P)	43	40	561	7.32×10^{-7}	1.88×10^{10}	56.2%
2 mol% Acetanilide (no US)	15.5 °C	105	54	7.01×10^{-7}	1.02×10^{9}	55.3%
2 mol% Metacetamol & Acetanilide (US 100% power)	34.4	37.3	346	1.19×10^{-7}	1.51×10^{10}	42.2%
2 mol% Metacetamol & Acetanilide (no US)	After maintaining at 15 °C for approx. 2.5 h	87–90	48	9.61×10^{-7}	1.14×10^{9}	32.0%
1 mol% Metacetamol & 1 mol% Acetanilide (50% US power)	44	87	61	7.19×10^{-7}	1.38×10^{9}	40.6%

3.3.1. Crystallisation Temperature

The nucleation temperature measured with and without the use of ultrasound for crystallisation of paracetamol in the presence of metacetamol and/or acetanilide is shown in Table 3. Even though nucleation is a stochastic process and some scatter may be anticipated among the measured data the experimental results clearly show that ultrasound has a significant effect on the nucleation process. For example, in the case of paracetamol crystallisation in the presence of 2% metacetamol, the ultrasound treated sample started to nucleate at around 36 °C, and was in the final stages of crystallisation by the time the suspension had been cooled to 15 °C. By contrast the sample not treated with ultrasound only started to nucleate after holding at 15 °C for approximately 1.5 h. This is believed to be due to the slow nucleation and crystal growth kinetics in the presence of impurities. Ultrasound can promote nucleation and generate substantial numbers of secondary nuclei from existing parent

crystals in the reactors. This is consistent with previous work [19,26,27,47] undertaken at different frequencies by different researchers. Although different frequencies have been employed and the intensity of cavitation is likely to have varied significantly between studies the research consistently shows that nucleation may be triggered at lower supersaturation levels and the nucleation rate may be increased with the use of ultrasound. There are two classical mechanisms of secondary nucleation (i) due to collisions between crystals and crystals colliding with the wall of the crystallizer or the agitator and (ii) removal of an ordered surface layer from the parent crystals due to fluid shear stresses. It is logical to anticipate that these phenomenon are amplified by application ultrasound. Cavitation occurring on, or near, crystal surfaces causes intense shear stresses which can lead to secondary nucleation [18,20,72,73]. It is suggested that ultrasound energy overcomes the kinetic barriers to nucleation by reducing the activation energy, and hence reducing the induction time. Ultrasound significantly decreased the metastable zone width, where the results indicate that the apparent order of primary nucleation is reduced and thus increases the solid precipitation rate [26]. During transient cavitation bubbles are formed and destroyed, this phenomenon creates localised supersaturation, which causes nucleation to occur. Similarly, the sonocrystallisation of mono and disaccharides from aqueous solution showed similar trends in a cooling crystallisation experiment, where ultrasound was applied, samples crystallised at higher temperature than in absence of ultrasound [46]. However, in another case, for amino acids the induction period increased with increasing ultrasonic irradiation energy up to a certain degree and subsequently decreased [74].

Crystal yield is calculated as the percentage of the mass of recovered product crystals following filtration washing and drying compared to the mass of input material. This contains an implicit assumption that there is no significant dissolution of crystals during washing which is justified based on the very low solubility of paracetamol in n-heptane, and the amount of paracetamol or impurities deposited from evaporation of retained wash liquor is negligible again due to the very low solubility. There are however product losses associated with material handling and with residues left on vessel walls and agitators. In addition some product losses are due to filtration and washing taking place at ambient temperature for reasons of practicality even though the crystallisation was halted at 15 °C. The typical estimated loss by these mechanisms is around 5%. The data in Table 2 indicate that intervention with ultrasound improves the product yield. In this series of experiments the yield is limited to 65% by the solubility at the isolation temperature based on the solubility in a pure system. The effect of impurities on the solubility at the isolation point has been shown to be negligible at the impurity concentrations investigated. For this reason, it is appropriate to use the same reference point to assess the yield in the experiments where impurities were present as it presents the yield with respect to a consistent baseline. The average yield for ultrasound treated samples is 50.7%, whereas for non-ultrasound treated samples the average yield is 45.2% (see Figure 5). This reduction in yield may be explained by considering the impact of ultrasound on several aspects of the crystallisation process. The non-ultrasound treated samples nucleate later in the process and the total number of nuclei is lower resulting in less surface area for growth and hence less opportunity for the solution to desupersaturate completely within the timeframe of the experiment. During crystal growth, enhanced local mass transfer arising from ultrasound irradiation increases the rate of mixing in the boundary layer, potentially accelerating the crystal growth process.

While it is well established that applying ultrasound to supersaturated solutions can initiate nucleation, the mechanism by which this takes place is not known. The bubble collapse associated with transient cavitation is reported to produce short lived and highly localised extremes of temperature and pressure which may contribute to a system overcoming energy barriers for nucleation. The passage of a sound wave is facilitated by molecular motion which may potentially promote cluster collisions which favours nucleation; however it may also serve to disrupt clusters. Cavitation events tend to be focused on discontinuities in the liquid phase and once crystals have formed these provide a readily available source of discontinuities which may act as cavitation centres and so contribute to the formation of new secondary nuclei. Prior to nucleation foreign particles such as dust are the principal source

of discontinuities which can act as sites for cavitation. Applying ultrasound during crystal growth speeds up the growth kinetics of crystals; several mechanisms can be proposed. Ultrasound enhances mixing [22,28,37,45,75] both through acoustic streaming and through the formation and subsequent collapse of cavitation bubbles which tend to be focused on existing crystals. These processes will enhance mass transfer within the boundary layer adjacent to the crystal. A further potential mechanism is the detachment of impurity molecules from the surface layer of the crystal eliminating the tendency for the impurities to block crystal growth. A consequence of the more complete de-supersaturation associated with insonation is that less solute remains in solution in the mother liquor. In combination, these processes triggered by insonation result in an increase of yield for the crystallisation process. Similarly, studies of crystallisation of lactose [42,55] showed the sonicated samples had higher yields than non-sonicated samples. This confirms that ultrasound can be applied to deliver a faster and more efficient crystallisation process.

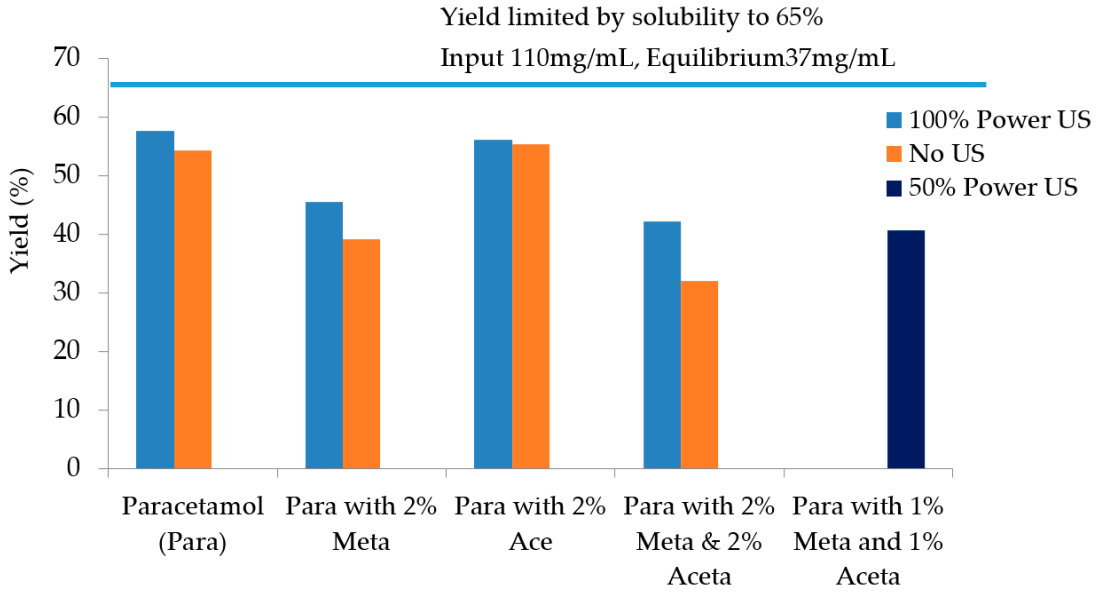

Figure 5. Yield of crystallisation with and without ultrasound in comparison with the yield limited by solubility to 65%, showing yield for the crystallisation process that approaches the equilibrium yield more closely with the use of ultrasound and that the presence of impurities impedes the desupersaturation process.

3.3.2. Crystal Size Distribution

The data presented in Figure 6 show that paracetamol crystallized in the presence of either of the impurities, metacetamol, acetanilide or both in combination has a narrower particle size distribution and a substantially larger number of smaller crystals when obtained with the use of ultrasound. For example, for the case of 2% of the impurity metacetamol, the sample treated with ultrasound at 100% power (1.45 ± 0.21 mW/cm^2) has a mean square weight (chord length) of 49 µm and many more particles than the corresponding sample which was not exposed to ultrasound which has a mean square weight of 109 µm. It is believed that application of ultrasound generates a substantial number of secondary nuclei which leads to a smaller product crystal size. Considering Figure 6a, it is noticeable that particle size distribution of the DOE centre point sample containing 1% of each of the impurities and subjected to the low (50% ultrasound power) is closer to the non insonated pure sample than the intensely insonated pure sample. This is consistent with both the impact of impurities inhibiting nucleation and growth combined with the low ultrasound intensity at the 50% power level (0.19 ± 0.06 mW/cm^2) compared with the high, 100% ultrasound power (1.45 ± 0.21 mW/cm^2).

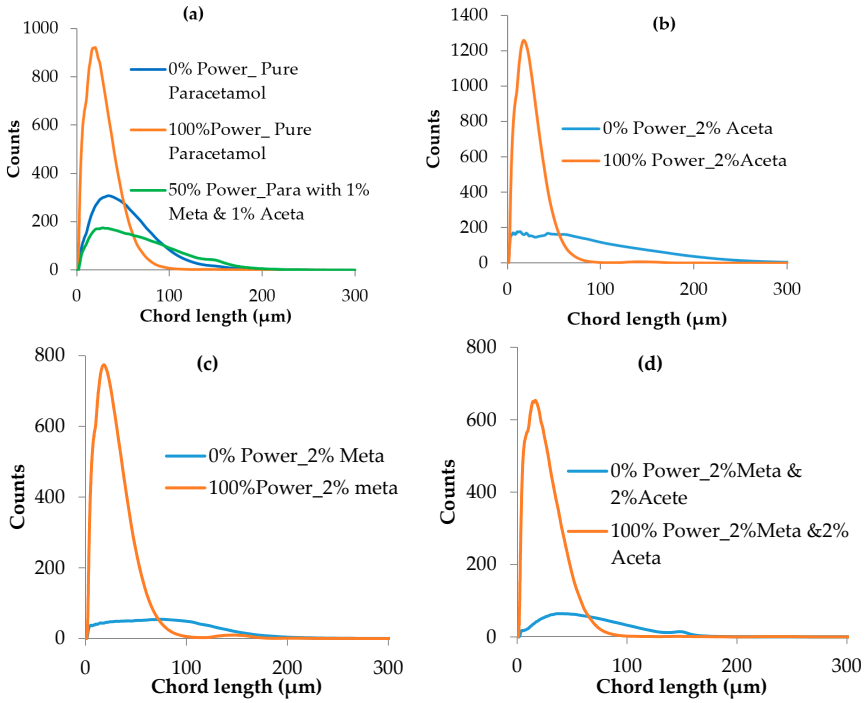

Figure 6. Particle size distribution of paracetamol crystals measured in situ at the end of crystallisation in the presence of impurities using an FBRM with and without the use of ultrasound (**a**) Pure paracetamol and 1% Metacetamol and 1% Acetanilide; (**b**) 2% acetanilide; (**c**) 2% Metacetamol; (**d**) both 2% Acetanilide and 2% Metacetamol.

Ultrasound has been reported to cause crystal breakage [20,37,39,76–78]. The breakage rate triggered by stable cavitation is reported to be independent of the applied power for paracetamol crystals with a median size (volume based distribution) of 75 µm and that a particle size threshold of ca. 35 µm exists. The particle size could not be reduced below this size regardless of the applied power or frequency. For transient cavitation, in contrast, higher powers lead to considerably smaller particles, with no threshold size within the investigated power range [79]. The effect is pronounced with a reduction in particle size of almost 70% compared to silent conditions is attained by using ultrasound [80]. It has been reported that low frequencies ($\leq$166 kHz) show a significant decrease in resultant particle size while high frequencies (>166 kHz) do not result in particle breakage [79].

The PSD in this study was compared to previous studies on paracetamol by Bhangu S. K. et al. [81] and with other organic materials which have been subject to ultrasonic irradiation (see Section S2 Supplementary data). The PSDs measured in situ at the end of crystallisation and prior to isolation were found to be consistent with literature data for the case of ultrasound assisted crystallisation of paracetamol [81].

3.3.3. Crystal Habit

Crystal habit has significant influence on the filtration washing and drying processes. It also plays a critical role in defining key physical properties of products including flow-ability and compressibility which are important in subsequent formulation processes. Figures 7 and 8 provide representative images of crystals of the isolated dry product. The ultrasound treated samples appear consistently smaller than the untreated product crystals, which is consistent with the measured PSD. The habit of crystals of paracetamol produced in this study is typically diamond shaped platelets regardless of whether they were produced with or without the use of ultrasound. The non-ultrasound treated samples showed the more consistent habit, which is similar to the commonly observed external morphology of the monoclinic form of paracetamol crystallised from pure IPA and with 1–2 mol%

metacetamol [5]. By contrast the ultrasound treated samples, contained particles which were more difficult to disperse; this is likely to be due to the much smaller crystals being more prone to agglomeration during drying. The crystal facets were also found to be damaged potentially due to increased particle breakage when subject to ultrasound particularly at the highest intensity. The images in Figure 8 for crystallisations taking place without ultrasonic intervention suggest that the crystals grown in the presence of impurities are better faceted than those grown from pure solution, this is consistent with the impact of impurities in slowing growth and yielding more visually perfect crystals. The crystal size is smaller with an impurity loading of 2% of both impurities compared to the case of 1% of both impurities. When ultrasound is applied the crystal size is more uniform but much smaller than in comparison to the experiments with no ultrasound. Lower ultrasound power level (50%) does not reduce crystal size as significantly relative to the experiments at 100% ultrasonic power level. This is consistent with the ultrasonic intensity data reported in Section 3.2.

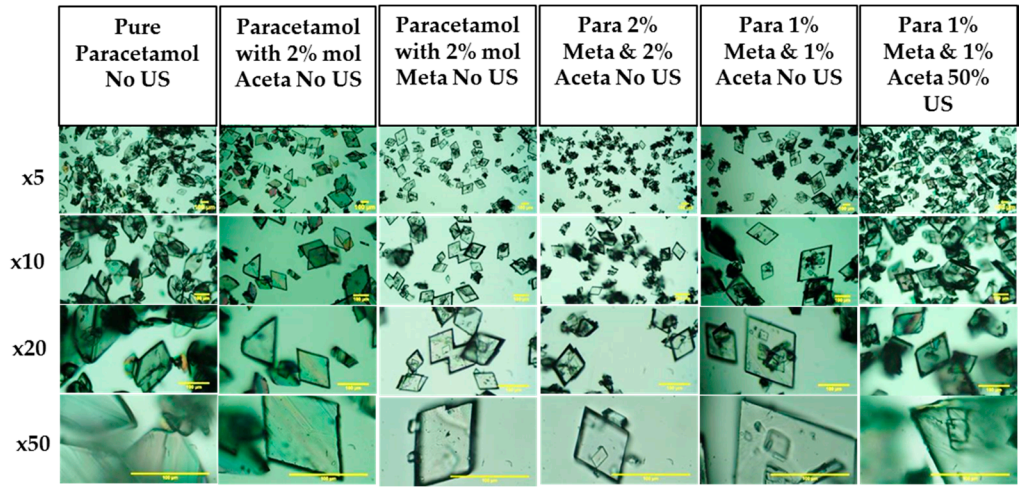

Figure 7. Optical microscopy images of recrystallized paracetamol crystal habit (from the left to the right) for the case of no added impurities with no US, with addition of 2% acetanilide with no US, with addition of 2% metacetamol with no US, with addition of 2% metacetamol and 2% acetanilide with no US, with addition of 1% metacetamol and 1% acetanilide with no US, with addition of 1% metacetamol and 1% acetanilide with 50% US power. Scale bar: 100 µm.

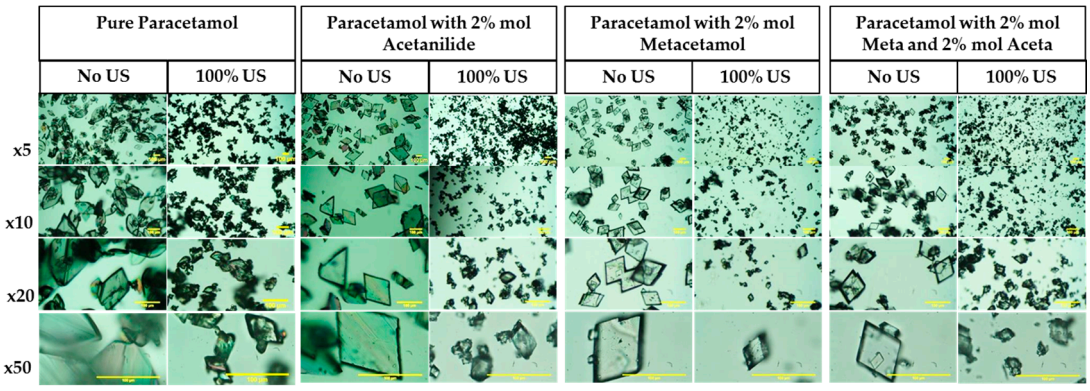

Figure 8. Optical microscopy images of recrystallized paracetamol crystal habit (from the left to the right) for the case of paracetamol with addition of 2% mol acetanilide with no US and 100% US power, paracetamol with addition of 2% mol metacetamol with no US and 100% US power, paracetamol with addition of 2% mol metacetamol and 2% mol acetanilide with no US and 100% US power. Scale bar: 100 µm.

3.3.4. Particle Isolation by Filtration

The paracetamol crystals were separated from their mother liquor after crystallisation by filtration. The crystallisation was scaled such that there was sufficient slurry to conduct three replicate experiments for each filtration. The variance in filtration rate provides an indication of the challenge associated with obtaining a representative suspension sample from a larger scale operation. The measured values are averaged across the replicate measurements to provide a representative measure of the filtration performance. The filtration data collected included filtration rate, filtration duration and filter cake resistance which are shown in Table 3 and Figure 9.

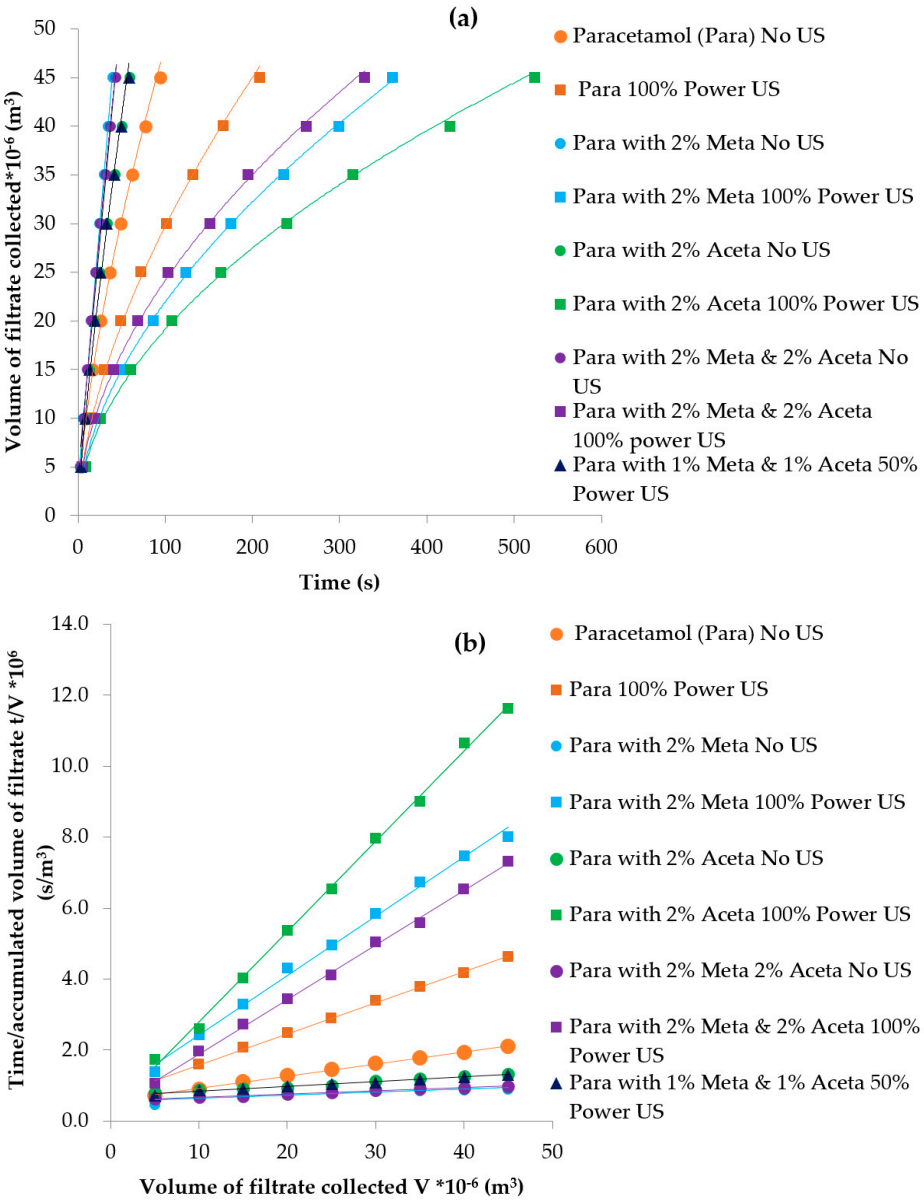

Figure 9. (**a**) Volume of filtrate collected versus time showing the filtration duration and filtration rate of ultrasound treated and non-ultrasound treated samples; (**b**) Plot of time/volume of filtrate collected (t/V) versus volume of filtrate (V) showing the ultrasound treated samples filter much more slowly and have correspondingly higher cake resistances (reported in Table 3) than the un-treated samples.

Comparing the ultrasound-treated and non-ultrasound treated samples, in the case of paracetamol crystallized from 2% metacetamol, the ultrasound treated sample had a filtration duration of 361 s

which is much longer than the 45 s taken by the non-ultrasound treated sample. This is consistent with the much smaller particle size distribution of the ultrasound treated sample this is supported both by FBRM and optical microscopy. The small crystals of the insonated sample pack to form a cake which contains relatively narrow pores between particles. This cake structure impedes the flow of filtrate through the cake compared with a cake formed of larger particles with correspondingly larger inter-particle pores. As a consequence, the filtration rates determined for the ultrasound treated samples are much lower than the non-ultrasound treated samples. In terms of cake resistance, the ultrasound treated samples exhibit a higher resistance compared with the non-ultrasound treated samples. For the non-ultrasound treated samples we can see that the gradient is around three times greater than the ultrasound treated samples (see Figure 9). As a result, the sample exhibits a higher cake resistance and thus increasing the filtration time. As particle size decreases, cake resistance increases, and cake filtration can result in excessively long filtration times. A second reason for the increase in filtration duration with ultrasound is that the yields are higher and hence the mass of material to be filtered is greater. For example in the case of the pure material and the sample with 2% acetanilide the yield is 54% and 55% respectively, whereas the samples containing 2% metacetamol and the combination of 2% metacetamol and 2% acetanilide have lower yields of 39% and 32% respectively. The lower yields are believed to be due to the impurities poisoning crystal growth.

The viscosity of the mother liquors was measured as a necessary parameter to apply Darcy's equation. The viscosity of the mother liquors was determined using a GV500 viscometer (Hydramotion Ltd., Malton, York, UK). A consistent value of 0.0057 Pa·s was recorded across all samples. The cake resistance was found to be in the range 1.5×10^{10} to 7.0×10^{11} kg/m for paracetamol with 2% of each impurity and the combination of 2% of both impurities for ultrasound treated samples and in the range of 9.0×10^{8} to 2.6×10^{9} kg/m for samples prepared in the absence of ultrasound and 50% power ultrasound treated samples. Insonication at the lower ultrasound power level (50%) has little effect on the crystal size. For the 50% power ultrasound treated samples this is consistent with the measured filtration duration and cake resistance.

From a formulation perspective it is often desirable to produce API crystals with a small particle size to achieve content uniformity in tablets and to enhance bioavailability, typically this is achieved by dry milling isolated product. The application of ultrasound leads to increased duration of isolation but this may offset against eliminating the additional processing step of size reduction.

3.3.5. Crystal Purity

One of the important success criteria for a crystallisation process is product purity. Each product sample was assayed by HPLC and the data is reported in Table 4.

Table 4. Summary of percentage of each compound in crystal product and in mother liquor.

Experiment Conditions	Compounds	Percentage of Compounds in Crystal Product (%)		Percentage of Compounds in Mother Liquor (%)	
		With US	No US	With US	No US
Pure Paracetamol	Paracetamol	100	100	100	100
	Metacetamol	0	0	0	0
	Acetanilide	0	0	0	0
Paracetamol with 2% Acetanilide	Paracetamol	99.62	99.15	94.65	96.02
	Acetanilide	0.35	0.85	5.35	3.98
Paracetamol with 2% Metacetamol	Paracetamol	98.47	98.12	96.05	96.43
	Metacetamol	1.52	1.88	3.95	3.57
Paracetamol with 2% Metacetamol and 2% Acetanilide	Paracetamol	98.1	97.98	91.37	91.49
	Metacetamol	1.19	1.44	3.91	3.92
	Acetanilide	0.55	0.58	4.72	4.59

The results show that the ultrasound treated product crystals contain less impurity than the non-insonated samples. This was the case for example with the paracetamol product isolated from

the 2% metacetamol solution where the concentration of the impurity in the product is reduced from 1.88% to 1.52%. Likewise the uptake of acetanilide from the 2% acetanilide crystallisation is reduced from 0.85% to 0.35%. The impurity analysis of the filtrate shows that more of the impurities remain in solution in the ultrasound treated samples. This result is more striking when the difference in particle size between the ultrasound treated and non-treated samples is considered. The ultrasonically treated products comprise far more smaller particles which have a much greater combined surface area on which impurities in the mother liquor may be retained and furthermore provide a larger washing challenge due to the finer pore structure and increased contact area between particles. Also, when the impurity loading in the crystallisation solution is highest the particle size is reduced to the larger extent, for example the case of 2% metacetamol and acetanilide.

Several mechanisms for impurity incorporation into crystalline products have been identified: (i) Surface adhesion/adsorption on the crystal surface; (ii) Bulk phase inclusion of mother liquor e.g., through agglomeration; (iii) inclusions of mother liquor within individual crystals and (iv) molecular substitution at the lattice sites. Potential purification methods for impurities in these different locations may be proposed. One mechanism by which the improvement in purity of crystals formed with continuous ultrasonic irradiation that can be proposed is that ultrasound produces very localised but short lived hot spots within the product crystal suspension. These hot spots are generated during the collapse of cavitation bubbles. Potentially this could provide sufficient perturbation to remove the mismatched impurity molecules from the product crystal lattice/surfaces due to the reduced binding energy associated with the different substrates. Another possible mechanism arises from reports that ultrasound may lead to a reduction in the formation of particle-particle agglomerates which in turn reduces the extent of agglomeration and so make the washing process more effective. A further observation is that, metacetmol appears to be more readily incorporated into the crystal product when compared to acetanilide. There may be several contributing causes for this segregation of the impurities (i) acetanilide is more soluble in 3-methyl 1-butanol than metacetamol; (ii) Metacetamol inhibits both nucleation and crystal growth more than acetanilide leading to reduced particle size making the filtration and washing process more challenging.

3.3.6. DoE and Multivariate Analysis

Using design of experiments, a multivariate approach, the combined effects of ultrasound power and impurity content on the crystallisation of paracetamol from 3-methyl 1-butanol were evaluated. Figure 10 shows both single factor and two factor effects on (a) Nucleation temperature; (b) Particle size; (c) Acetanilide incorporation; (d) Metacetamol incorporation and (e) Yield. From this it is clear that ultrasound plays a dominant role in triggering nucleation at higher temperatures (a) and reducing the mean particle size (b), is has a more modest effect in increasing yield (e) where the dominant effect is the presence of metacetamol. As expected the principal factor influencing the amount of impurity in the product is the impurity concentration is the feed solution (c-acetanilide) and (d-metacetamol). Most two factor effects are relatively modest.

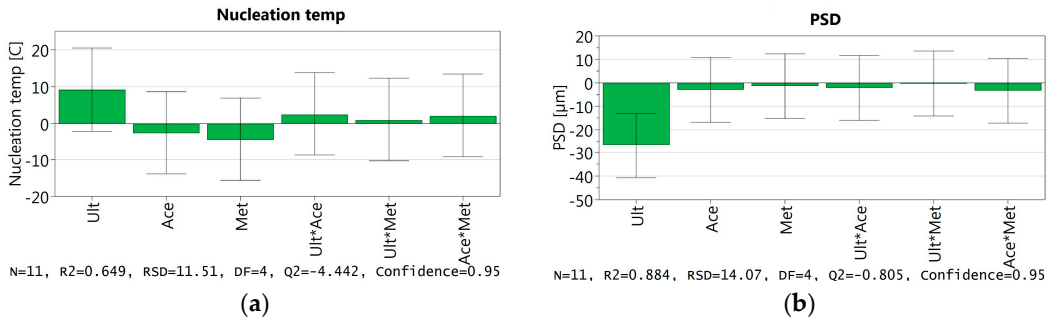

Figure 10. *Cont.*

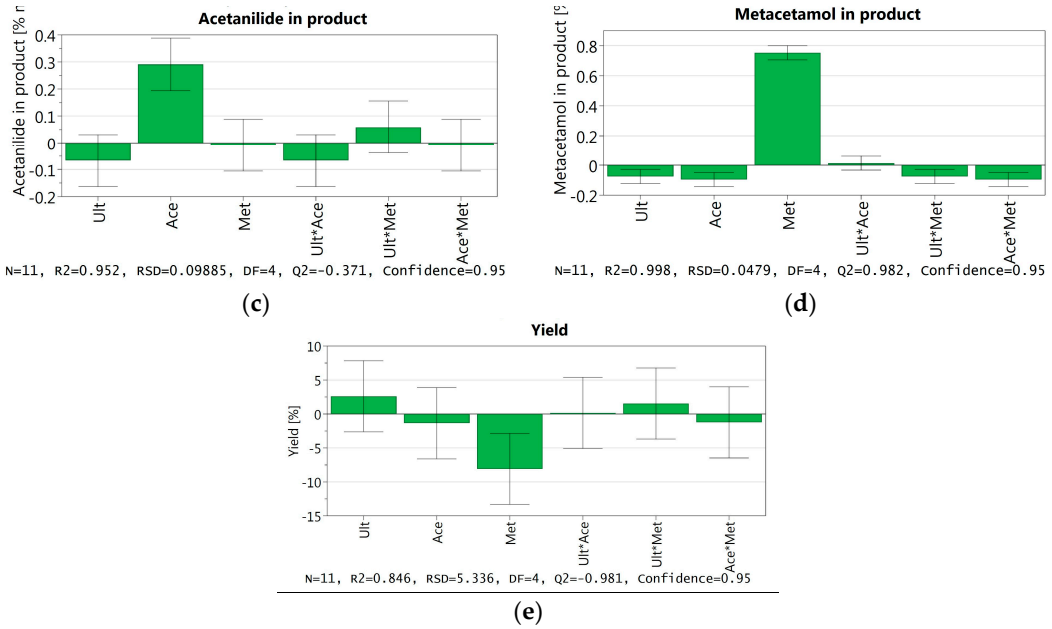

Figure 10. Effect of coefficients (using MLR model) from DoE showing the extent of the effect of factors on the responds; nucleation temperature (**a**), PSD (**b**), acetanilide in product (**c**), metacetamol in product (**d**), and yield (**e**).

The Figure 11a–e provides further detail of the predicted impact of the experimental factors, for example Figure 11a,b reveal that the difference in nucleation temperature between the least and most forcing conditions exceeds 20 °C. Comparing Figure 11c,d show that ultrasound is the dominant variable in modifying particle size. Figure 11e,f show that the presence of acetanilide has little impact on yield whereas metacetamol has a significant effect, reducing yield by around 25%. Figure 11g,h show the effect of insonation on isolated product purity, it is readily apparent that ultrasound has a significant effect in reducing acetanilide incorporation into the product but is less effective in reducing the level of metacetamol incorporation.

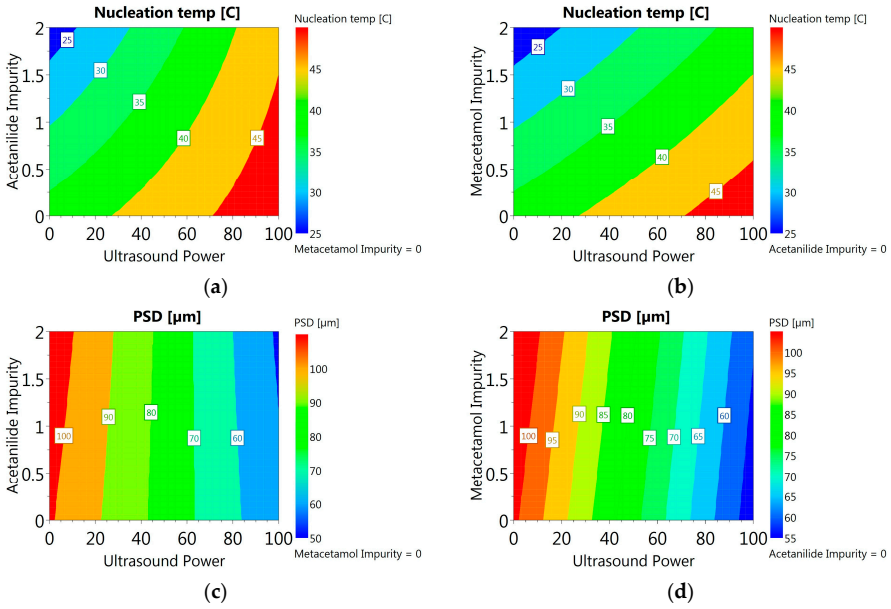

Figure 11. *Cont.*

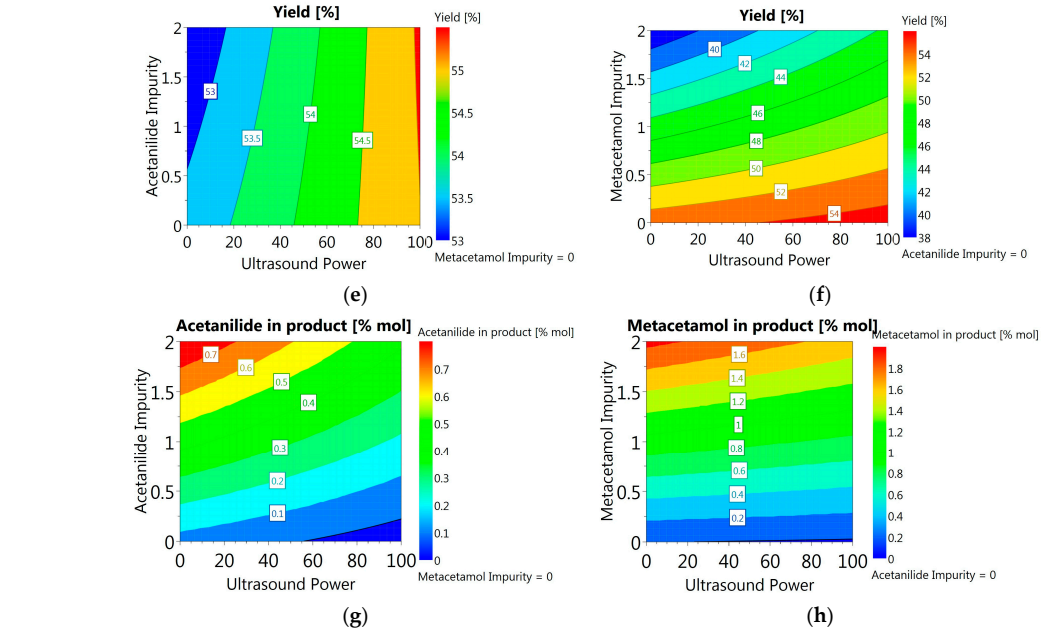

Figure 11. Response contour plot showing effect of ultrasound power (from 0 to 100% ultrasonic power), acetanilide and metacetamol impurity (0 to 2% mol) on nucleation temperature (**a**,**b**), PSD (**c**,**d**), yield (**e**,**f**) and the percentage of impurities in crystal product (**g**,**h**).

The combined effects are represented in Figure 12 which allows the relative magnitude of ultrasound and the two impurities on PSD, yield and nucleation temperature to be assessed.

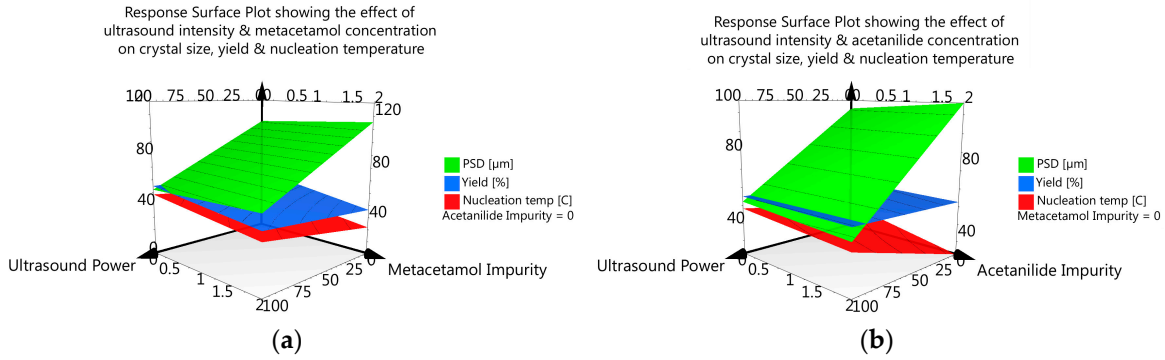

Figure 12. Respond surface plot showing the effect of ultrasound intensity, metacetamol (**a**) and acetanilide (**b**) concentration on crystal size, yield and nucleation temperature.

4. Discussion

The nucleation point recorded in the 150 mL flasks for the non-sononucleated samples are in good agreement with one another; there is some variability which is consistent with the stochastic nature of nucleation. For pure paracetamol, the sub-cooling required to induce nucleation in the absence of ultrasound is around 30 °C. It has been shown that metacetamol has a more significant effect on metastable zone width than acetanilide causing increased induction time.

Due to the earlier nucleation point and larger number of nuclei in the sononucleated samples the available surface area for growth is greater than in the non-sononucleated samples, this has an impact throughout the subsequent crystallisation and isolation. There is a strong link between ultrasound effects on nucleation kinetics, product crystal size distribution, filtration rate and product purity. The principal attribute of the crystals which affects filtration performance is the crystal-size

distribution. At the maximum (100%) ultrasonic intensity some evidence of crystal damage is seen in the photomicrographs. In terms of product crystal purity, several mechanisms of impurity incorporation have been identified; adhesion/adsorption on crystal faces; bulk inclusion of mother liquor entrapped between particles; inclusions of mother liquor within individual crystals; molecular substitution within the lattice and incomplete removal of mother liquors during washing. In this bulk crystallisation investigation evidence has been gathered which suggests that ultrasonic intervention does lead to higher crystal purity. However it has not been possible to attribute specific quantities of the overall impurity loading between these different mechanisms.

The proposed mechanism for the effects seen in the present work involves (i) Crystal growth is the selective process through which growing crystal recognizes the host and rejects impurities. Since the impurity molecules differ from the host molecules, they do not fit the growth site as easily as the host (solute) molecules. The greater the structural similarity between impurity and host molecules, the more readily the impurity molecules incorporate into the crystal lattice. During the growth process when impurities arrive at the crystal surface, they diffuse across the surface until they access a position with a sufficiently strong binding interaction that they attach to, and become incorporated into the lattice. If ultrasound is applied at an appropriate intensity, frequency and duration, it is proposed that the molecular motion and fluctuation in pressure and temperature associated with the passage of the ultrasound wave may replace the molecules in the boundary layer surrounding the crystal with molecules from the bulk solution. At ultrasound intensities above the cavitation threshold it is proposed that the shockwave and associated local heating arising from the collapse of a cavitation bubble disturbs the local equilibrium at the liquid/solid interface and may selectively remove impurity molecules from the crystal surface due to weaker binding energy associated with the imperfect fit to the lattice. (ii) In addition, when sonocrystallisation is employed, nucleation is initiated at lower supersaturations than would be the case without ultrasonic intervention. As a consequence, more of the crystal growth takes place at lower supersaturation levels than in a spontaneously nucleated crystallisation, during growth at lower supersaturation the crystal faces tend to be smoother, and the rate of growth lower, providing increased opportunity for impurity molecule removal from growth sites prior them being overgrown and hence built into the bulk of the crystal resulting in less impurity becoming incorporated into the final product. (iii) Ultrasound increased molecular motion adjacent to the growing crystal improving transport to and from the crystal faces. Highly localised perturbations caused by cavitation events lead to momentary local temperature fluctuations. When these occur close to strained regions of the lattice where impurities are attached they favour release of the impurity molecules. While these hypotheses are plausible the experimental evidence gathered here does not provide significant further mechanistic clarification.

5. Conclusions

The effect of sono-crystallisation on paracetamol product purity has been demonstrated for two structurally similar impurities. The classic benefits reported for sono-crystallisation; acceleration of nucleation, modification of crystal size distribution, and enhancement of yield have been confirmed. The work has added another dimension, that ultrasound intervention during crystallisation in the presence of impurities can enhance product crystal purity. However, the underlying mechanisms of this effect are not yet well understood.

These findings provide convincing evidence for the potential application of ultrasound to other organic systems to enhance purification. Through this work, an insight into the possibilities of enhancing purity of pharmaceutical products by sonocrystallisation has been demonstrated.

Supplementary Materials: The following are available online at www.mdpi.com/2073-4352/7/10/294/s1, Section S1: Data related to solubility of paracetamol, metacetamol and acetanilide in 3-methyl-1-butanol, Section S2: Comparison of the mean PSD of paracetamol nucleated and grown in the presence of structurally similar impurities (this work) with the PSD of some organic materials obtained from sonocrystallisation from literature.

Acknowledgments: The authors gratefully acknowledge the financial support of the EPSRC research grant EP/L014971/1, "Transforming industrial crystallisation by sono-mechanical manipulation of crystal surfaces" the Department of Chemical and Process Engineering, University of Strathclyde by EPSRC; and the EPSRC Centre for Innovative Manufacturing in Continuous Manufacturing and Crystallisation (CMAC) National Facility laboratories, housed within the University of Strathclyde's Technology and Innovation Centre, for the lab facility. We also thank the Astra Zeneca for the HPLC method for analysis of paracetamol and related impurities.

Author Contributions: Thai T. H. Nguyen and Chris J. Price conceived and designed the sono-crystallisation experiments; Thai T. H. Nguyen and Azeem Khan performed the sono-crystallisation experiments and analyzed the data; Layla M. Bruce performed the solubility measurements (using gravimetric method) and Thai T. H. Nguyen performed the solubility measurements (using detection of the dissolution temperature method); Richard L. O'Leary and Clarissa Forbes designed and performed the ultrasonic intensity measurements; Thai T. H. Nguyen and Chris J. Price wrote the paper.

Conflicts of Interest: The authors declare no conflict of interest.

References

1. Beckmann, W. *Crystallization: Basic Concepts and Industrial Applications*; John Wiley & Sons: Hoboken, NJ, USA, 2013.
2. Hendriksen, B.A.; Grant, D.J.; Meenan, P.; Green, D.A. Crystallisation of paracetamol (acetaminophen) in the presence of structurally related substances. *J. Cryst. Growth* **1998**, *183*, 629–640. [CrossRef]
3. Prasad, K.V.; Ristic, R.I.; Sheen, D.B.; Sherwood, J.N. Crystallization of paracetamol from solution in the presence and absence of impurity. *Int. J. Pharm.* **2001**, *215*, 29–44. [CrossRef]
4. Thompson, C.; Davies, M.C.; Roberts, C.J.; Tendler, S.J.B.; Wilkinson, M.J. The effects of additives on the growth and morphology of paracetamol (acetaminophen) crystals. *Int. J. Pharm.* **2004**, *280*, 137–150. [CrossRef] [PubMed]
5. Saleemi, A.; Onyemelukwe, I.I.; Nagy, Z. Effects of a structurally related substance on the crystallization of paracetamol. *Front. Chem. Sci. Eng.* **2013**, *7*, 79–87. [CrossRef]
6. Hendriksen, B.A.; Grant, D.J. The effect of structurally related substances on the nucleation kinetics of paracetamol (acetaminophen). *J. Cryst. Growth* **1995**, *156*, 252–260. [CrossRef]
7. Rauls, M.; Bartosch, K.; Kind, M.; Kuch, S.; Lacmann, R.; Mersmann, A. The influence of impurities on crystallization kinetics–A case study on ammonium sulfate. *J. Cryst. Growth* **2000**, *213*, 116–128. [CrossRef]
8. Sangwal, K.; Mielniczek-Brzoska, E. Effect of impurities on metastable zone width for the growth of ammonium oxalate monohydrate crystals from aqueous solutions. *J. Cryst. Growth* **2004**, *267*, 662–675. [CrossRef]
9. Podder, J. The study of impurities effect on the growth and nucleation kinetics of potassium dihydrogen phosphate. *J. Cryst. Growth* **2002**, *237*, 70–75. [CrossRef]
10. Poornachary, S.K.; Lau, G.; Chow, P.S.; Tan, R.B.H.; George, N. The Effect and Counter-Effect of Impurities on Crystallization of an Agrochemical Active Ingredient: Stereochemical Rationalization and Nanoscale Crystal Growth Visualization. *Cryst. Growth Des.* **2011**, *11*, 492–500. [CrossRef]
11. Mukuta, T.; Lee, A.Y.; Kawakami, T.; Myerson, A.S. Influence of impurities on the solution-mediated phase transformation of an active pharmaceutical ingredient. *Cryst. Growth Des.* **2005**, *5*, 1429–1436. [CrossRef]
12. Févotte, F.; Févotte, G. A method of characteristics for solving population balance equations (PBE) describing the adsorption of impurities during crystallization processes. *Chem. Eng. Sci.* **2010**, *65*, 3191–3198. [CrossRef]
13. Judge, R.A.; Forsythe, E.L.; Pusey, M.L. The effect of protein impurities on lysozyme crystal growth. *Biotechnol. Bioeng.* **1998**, *59*, 776–785. [CrossRef]
14. Sangwal, K. Effects of impurities on crystal growth processes. *Prog. Cryst. Growth Charact. Mater.* **1996**, *32*, 3–43. [CrossRef]
15. Scott, C.; Black, S. In-line analysis of impurity effects on crystallisation. *Org. Process Res. Dev.* **2005**, *9*, 890–893. [CrossRef]
16. Poornachary, S.K.; Chow, P.S.; Tan, R.B. Effect of solution speciation of impurities on α-glycine crystal habit: A molecular modeling study. *J. Cryst. Growth* **2008**, *310*, 3034–3041. [CrossRef]
17. Repic, O. *Principles of Process Research and Chemical Development in the Pharmaceutical Industry*; John Wiley & Sons: Hoboken, NJ, USA, 1998.
18. Chow, R.; Blindt, R.; Chivers, R.; Povey, M. A study on the primary and secondary nucleation of ice by power ultrasound. *Ultrasonics* **2005**, *43*, 227–230. [CrossRef] [PubMed]

19. Crespo, R.; Martins, P.M.; Gales, L.; Rocha, F.; Damas, A.M. Potential use of ultrasound to promote protein crystallization. *J. Appl. Crystallogr.* **2010**, *43*, 1419–1425. [CrossRef]
20. Devarakonda, S.; Evans, J.M.B.; Myerson, A.S. Impact of Ultrasonic Energy on the Crystallization of Dextrose Monohydrate. *Cryst. Growth Des.* **2003**, *3*, 741–746. [CrossRef]
21. Dodds, J.; Espitalier, F.; Louisnard, O.; Grossier, R.; David, R.; Hassoun, M.; Baillon, F.; Gatumel, C.; Lyczko, N. The Effect of Ultrasound on Crystallisation-Precipitation Processes: Some Examples and a New Segregation Model. *Part. Part. Syst. Charact.* **2007**, *24*, 18–28. [CrossRef]
22. Guo, Z.; Zhang, M.; Li, H.; Wang, J.; Kougoulos, E. Effect of ultrasound on anti-solvent crystallization process. *J. Cryst. Growth* **2005**, *273*, 555–563. [CrossRef]
23. Higaki, K.; Ueno, S.; Koyano, T.; Sato, K. Effects of ultrasonic irradiation on crystallization behavior of tripalmitoylglycerol and cocoa butter. *J. Am. Oil Chem. Soc.* **2001**, *78*, 513–518. [CrossRef]
24. Kordylla, A.; Koch, S.; Tumakaka, F.; Schembecker, G. Towards an optimized crystallization with ultrasound: Effect of solvent properties and ultrasonic process parameters. *J. Cryst. Growth* **2008**, *310*, 4177–4184. [CrossRef]
25. De Castro, M.D.L.; Priego-Capote, F. Ultrasound-assisted crystallization (sonocrystallization). *Ultrason. Sonochem.* **2007**, *14*, 717–724.
26. Lyczko, N.; Espitalier, F.; Louisnard, O.; Schwartzentruber, J. Effect of ultrasound on the induction time and the metastable zone widths of potassium sulphate. *Chem. Eng. J.* **2002**, *86*, 233–241. [CrossRef]
27. Miyasaka, E.; Kato, Y.; Hagisawa, M.; Hirasawa, I. Effect of ultrasonic irradiation on the number of acetylsalicylic acid crystals produced under the supersaturated condition and the ability of controlling the final crystal size via primary nucleation. *J. Cryst. Growth* **2006**, *289*, 324–330. [CrossRef]
28. Narducci, O.; Jones, A.G.; Kougoulos, E. Continuous crystallization of adipic acid with ultrasound. *Chem. Eng. Sci.* **2011**, *66*, 1069–1076. [CrossRef]
29. Nývlt, J.; Žáček, S. Effect of Ultrasonics on Agglomeration. *Cryst. Res. Technol.* **1995**, *30*, 1055–1063. [CrossRef]
30. Patrick, M.; Blindt, R.; Janssen, J. The effect of ultrasonic intensity on the crystal structure of palm oil. *Ultrason. Sonochem.* **2004**, *11*, 251–255. [CrossRef] [PubMed]
31. Ramisetty, K.A.; Pandit, A.B.; Gogate, P.R. Ultrasound-Assisted Antisolvent Crystallization of Benzoic Acid: Effect of Process Variables Supported by Theoretical Simulations. *Ind. Eng. Chem. Res.* **2013**, *52*, 17573–17582. [CrossRef]
32. Sayan, P.; Sargut, S.T.; Kiran, B. Effect of ultrasonic irradiation on crystallization kinetics of potassium dihydrogen phosphate. *Ultrason. Sonochem.* **2011**, *18*, 795–800. [CrossRef] [PubMed]
33. Virone, C.; Kramer, H.J.M.; van Rosmalen, G.M.; Stoop, A.H.; Bakker, T.W. Primary nucleation induced by ultrasonic cavitation. *J. Cryst. Growth* **2006**, *294*, 9–15. [CrossRef]
34. Boels, L.; Wagterveld, R.M.; Mayer, M.J.; Witkamp, G.J. Seeded calcite sonocrystallization. *J. Cryst. Growth* **2010**, *312*, 961–966. [CrossRef]
35. Dhumal, R.; Biradar, S.; Paradkar, A.; York, P. Ultrasound Assisted Engineering of Lactose Crystals. *Pharm. Res.* **2008**, *25*, 2835–2844. [CrossRef] [PubMed]
36. Eder, R.J.P.; Schrank, S.; Besenhard, M.O.; Roblegg, E.; Gruber-Woelfler, H.; Khinast, J.G. Continuous Sonocrystallization of Acetylsalicylic Acid (ASA): Control of Crystal Size. *Cryst. Growth Des.* **2012**, *12*, 4733–4738. [CrossRef]
37. Guo, Z.; Jones, A.G.; Li, N.; Germana, S. High-speed observation of the effects of ultrasound on liquid mixing and agglomerated crystal breakage processes. *Powder Technol.* **2007**, *171*, 146–153. [CrossRef]
38. Kim, S.; Wei, C.; Kiang, S. Crystallization process development of an active pharmaceutical ingredient and particle engineering via the use of ultrasonics and temperature cycling. *Org. Process Res. Dev.* **2003**, *7*, 997–1001. [CrossRef]
39. Kougoulos, E.; Marziano, I.; Miller, P.R. Lactose particle engineering: Influence of ultrasound and anti-solvent on crystal habit and particle size. *J. Cryst. Growth* **2010**, *312*, 3509–3520. [CrossRef]
40. Li, H.; Wang, J.; Bao, Y.; Guo, Z.; Zhang, M. Rapid sonocrystallization in the salting-out process. *J. Cryst. Growth* **2003**, *247*, 192–198. [CrossRef]
41. Nalajala, V.S.; Moholkar, V.S. Investigations in the physical mechanism of sonocrystallization. *Ultrason. Sonochem.* **2011**, *18*, 345–355. [CrossRef] [PubMed]
42. Patel, S.R.; Murthy, Z.V.P. Effect of process parameters on crystal size and morphology of lactose in ultrasound-assisted crystallization. *Cryst. Res. Technol.* **2011**, *46*, 243–248. [CrossRef]

43. Wohlgemuth, K.; Kordylla, A.; Ruether, F.; Schembecker, G. Experimental study of the effect of bubbles on nucleation during batch cooling crystallization. *Chem. Eng. Sci.* **2009**, *64*, 4155–4163. [CrossRef]
44. Amara, N.; Ratsimba, B.; Wilhelm, A.-M.; Delmas, H. Crystallization of potash alum: Effect of power ultrasound. *Ultrason. Sonochem.* **2001**, *8*, 265–270. [CrossRef]
45. Li, H.; Li, H.; Guo, Z.; Liu, Y. The application of power ultrasound to reaction crystallization. *Ultrason. Sonochem.* **2006**, *13*, 359–363. [CrossRef] [PubMed]
46. Ruecroft, G.; Hipkiss, D.; Ly, T.; Maxted, N.; Cains, P.W. Sonocrystallization: The Use of Ultrasound for Improved Industrial Crystallization. *Org. Process Res. Dev.* **2005**, *9*, 923–932. [CrossRef]
47. Gracin, S.; Uusi-Penttilä, M.; Rasmuson, Å.C. Influence of Ultrasound on the Nucleation of Polymorphs of p-Aminobenzoic Acid. *Cryst. Growth Des.* **2005**, *5*, 1787–1794. [CrossRef]
48. Louhi-Kultanen, M.; Karjalainen, M.; Rantanen, J.; Huhtanen, M.; Kallas, J. Crystallization of glycine with ultrasound. *Int. J. Pharm.* **2006**, *320*, 23–29. [CrossRef] [PubMed]
49. Srinivasan, R.; Shirgaonkar, I.Z.; Pandit, A.B. Effect of Sonication on Crystal Properties. *Sep. Sci. Technol.* **1995**, *30*, 2239–2243. [CrossRef]
50. Suslick, K.S. The chemical effects of ultrasound. *Sci. Am.* **1989**, *260*, 80–86. [CrossRef]
51. Apfel, R.E. Sonic effervescence: A tutorial on acoustic cavitation. *J. Acoust. Soc. Am.* **1997**, *101*, 1227–1237. [CrossRef]
52. Lauterborn, W.; Ohl, C.-D. Cavitation bubble dynamics. *Ultrason. Sonochem.* **1997**, *4*, 65–75. [CrossRef]
53. Lauterborn, W.; Kurz, T.; Mettin, R.; Ohl, C. Experimental and theoretical bubble dynamics. *Adv. Chem. Phys.* **1999**, *110*, 295–380.
54. Price, C.J. Take some solid steps to improve crystallization. *Chem. Eng. Prog.* **1997**, *93*, 34–43.
55. Zamanipoor, M.H.; Mancera, R.L. The emerging application of ultrasound in lactose crystallisation. *Trends Food Sci. Technol.* **2014**, *38*, 47–59. [CrossRef]
56. Knorr, D.; Zenker, M.; Heinz, V.; Lee, D.-U. Applications and potential of ultrasonics in food processing. *Trends Food Sci. Technol.* **2004**, *15*, 261–266. [CrossRef]
57. Mason, T.; Paniwnyk, L.; Lorimer, J. The uses of ultrasound in food technology. *Ultrason. Sonochem.* **1996**, *3*, S253–S260. [CrossRef]
58. Jiang, M.; Papageorgiou, C.D.; Waetzig, J.; Hardy, A.; Langston, M.; Braatz, R.D. Indirect ultrasonication in continuous slug-flow crystallization. *Cryst. Growth Des.* **2015**, *15*, 2486–2492. [CrossRef]
59. Rossi, D.; Jamshidi, R.; Saffari, N.; Kuhn, S.; Gavriilidis, A.; Mazzei, L. Continuous-flow sonocrystallization in droplet-based microfluidics. *Cryst. Growth Des.* **2015**, *15*, 5519–5529. [CrossRef]
60. Siddique, H.; Brown, C.J.; Houson, I.; Florence, A.J. Establishment of a Continuous Sonocrystallization Process for Lactose in an Oscillatory Baffled Crystallizer. *Org. Process Res. Dev.* **2015**, *19*, 1871–1881. [CrossRef]
61. Haisa, M.; Kashino, S.; Kawai, R.; Maeda, H. The Monoclinic Form of p-Hydroxyacetanilide. *Acta Crystallogr. B* **1976**, *32*, 1283–1285. [CrossRef]
62. Haisa, M.; Kashino, S.; Maeda, H. The orthorhombic form of p-hydroxyacetanilide. *Acta Crystallogr. B* **1974**, *30*, 2510–2512. [CrossRef]
63. Perrin, M.-A.; Neumann, M.A.; Elmaleh, H.; Zaske, L. Crystal structure determination of the elusive paracetamol Form III. *Chem. Commun.* **2009**, 3181–3183. [CrossRef] [PubMed]
64. Ristic, R.; Finnie, S.; Sheen, D.; Sherwood, J. Macro-and micromorphology of monoclinic paracetamol grown from pure aqueous solution. *J. Phys. Chem. B* **2001**, *105*, 9057–9066. [CrossRef]
65. Ripperger, S.; Gösele, W.; Alt, C.; Loewe, T. Filtration, 1. fundamentals. In *Ullmann's Encyclopedia of Industrial Chemistry*; John Wiley & Sons: Hoboken, NJ, USA, 2009; Volume 14, pp. 677–709.
66. Behera, S.; Ghanty, S.; Ahmad, F.; Santra, S.; Banerjee, S. UV-visible spectrophotometric method development and validation of assay of paracetamol tablet formulation. *Int. J. Chem. Anal. Sci.* **2012**, *3*, 2–6. [CrossRef]
67. Ungnade, H.E. Ultraviolet Absorption Spectra of Acetanilides. *J. Am. Chem. Soc.* **1954**, *76*, 5133–5135. [CrossRef]
68. Granberg, R.A.; Rasmuson, Å.C. Solubility of Paracetamol in Pure Solvents. *J. Chem. Eng. Data* **1999**, *44*, 1391–1395. [CrossRef]
69. Baena, Y.; Pinzón, J.A.; Barbosa, H.J.; Martínez, F. Temperature-dependence of the solubility of some acetanilide derivatives in several organic and aqueous solvents. *Phys. Chem. Liq.* **2004**, *42*, 603–613. [CrossRef]

70. Barrio, M.; Huguet, J.; Rietveld, I.B.; Robert, B.; Céolin, R.; Tamarit, J.-L. The Pressure-Temperature Phase Diagram of Metacetamol and Its Comparison to the Phase Diagram of Paracetamol. *J. Pharm. Sci.* **2017**, *106*, 1538–1544. [CrossRef] [PubMed]
71. Drebushchak, V.A.; McGregor, L.; Rychkov, D.A. Cooling rate "window" in the crystallization of metacetamol form II. *J. Therm. Anal. Calorim.* **2017**, *127*, 1807–1814. [CrossRef]
72. Chow, R.; Blindt, R.; Kamp, A.; Grocutt, P.; Chivers, R. The microscopic visualisation of the sonocrystallisation of ice using a novel ultrasonic cold stage. *Ultrason. Sonochem.* **2004**, *11*, 245–250. [CrossRef] [PubMed]
73. Chow, R.; Blindt, R.; Chivers, R.; Povey, M. The sonocrystallisation of ice in sucrose solutions: Primary and secondary nucleation. *Ultrasonics* **2003**, *41*, 595–604. [CrossRef] [PubMed]
74. Kurotani, M.; Miyasaka, E.; Ebihara, S.; Hirasawa, I. Effect of ultrasonic irradiation on the behavior of primary nucleation of amino acids in supersaturated solutions. *J. Cryst. Growth* **2009**, *311*, 2714–2721. [CrossRef]
75. Dhumal, R.S.; Biradar, S.V.; Paradkar, A.R.; York, P. Particle engineering using sonocrystallization: Salbutamol sulphate for pulmonary delivery. *Int. J. Pharm.* **2009**, *368*, 129–137. [CrossRef] [PubMed]
76. Raman, V.; Abbas, A. Experimental investigations on ultrasound mediated particle breakage. *Ultrason. Sonochem.* **2008**, *15*, 55–64. [CrossRef] [PubMed]
77. Wagterveld, R.; Boels, L.; Mayer, M.; Witkamp, G. Visualization of acoustic cavitation effects on suspended calcite crystals. *Ultrason. Sonochem.* **2011**, *18*, 216–225. [CrossRef] [PubMed]
78. Sander, J.R.; Zeiger, B.W.; Suslick, K.S. Sonocrystallization and sonofragmentation. *Ultrason. Sonochem.* **2014**, *21*, 1908–1915. [CrossRef] [PubMed]
79. Jordens, J. Application of Acoustic Energy in Crystallization Processes. Ph.D. Thesis, KU Leuven, Leuven, Belgium, 2016.
80. Gielen, B.; Kusters, P.; Jordens, J.; Thomassen, L.C.J.; Van Gerven, T.; Braeken, L. Energy efficient crystallization of paracetamol using pulsed ultrasound. *Chem. Eng. Process. Process Intensif.* **2017**, *114*, 55–66. [CrossRef]
81. Kaur Bhangu, S.; Ashokkumar, M.; Lee, J. Ultrasound Assisted Crystallization of Paracetamol: Crystal Size Distribution and Polymorph Control. *Cryst. Growth Des.* **2016**, *16*, 1934–1941. [CrossRef]

© 2017 by the authors. Licensee MDPI, Basel, Switzerland. This article is an open access article distributed under the terms and conditions of the Creative Commons Attribution (CC BY) license (http://creativecommons.org/licenses/by/4.0/).